Gel-based drug delivery for safe and effective cancer immunotherapy

Chung, C.K.

2

CHAPTER 2

Thermosensitive hydrogels as sustained drug delivery system for CTLA-4 checkpoint blocking antibodies

Chih Kit Chung, Marieke F. Fransen, Koen van der Maaden, Yaima Campos, Jomarien García-Couce, Dana Kralisch, Alan Chan, Ferry Ossendorp and Luis J. Cruz

Journal of Controlled Release.
2020 Jul 10; 323:1-11. 10.1016/j.jconrel.2020.03.050.

Abstract

Thermosensitive poloxamer 407 (P407) hydrogels were evaluated as slow release system for optimizing CTLA-4 therapy. Slow release reduces systemic antibody levels and potentially mitigates the side effects of CTLA-4 therapy. The 25% P407 hydrogel is injectable at room temperature and depots are established quickly after subcutaneous injection. Scanning electron microscopy revealed the porous structure of the hydrogel, average pore surface was 1335 μm^2. Release studies were optimized using the human IgG antibody. IgG was easily incorporated in the hydrogel by simple mixing and no antibodies were lost during preparation. In vitro, hydrogels showed low burst release within the first 24 h. Total IgG load was gradually released within 120 h. In vitro cytotoxicity assays showed that P407 is not cytotoxic and induces no immune activation by itself. In vivo, P407 hydrogels significantly reduced serum IgG levels, were biocompatible and were broken down 1 week after injection. Finally, local hydrogel delivery of anti-CTLA-4 antibodies near established tumors effectively slow down tumor growth, whilst significantly reducing serum anti-CTLA-4 levels. Altogether, P407 hydrogels represent a promising delivery system for the optimization of CTLA-4 blocking therapy.

Keywords: Cytotoxic T-lymphocyte-associated protein 4; hydrogel; immune checkpoint blockade; immune related adverse event; poloxamer; sustained release.

1. Introduction

The potential of CTLA-4 (cytotoxic T-lymphocyte-associated protein 4) blockade to confer durable response rates in cancer patients has become increasingly evident[1, 2]. CTLA-4 belongs to the category inhibitory checkpoint molecules, which can be exploited for generating anti-tumor immune responses[3, 4]. It is expressed profoundly on activated T-helper 1 cells (TH1) and cytotoxic T lymphocytes (CTLs). Upon binding the antigen presenting cell (APC) co-stimulatory molecules CD80 and CD86, CTLA-4 transmits inhibitory signals, which lead to cessation of T cell activation and proliferation[5]. As such, blocking the CTLA-4 receptor and its associated immune pathways might unleash anti-tumor immunity, thereby keeping tumor growth in check. Phase II/III trials have indeed demonstrated robust therapeutic effects of Ipilimumab in notably advanced staged melanomas[6-9], which have further endorsed the optimization of CTLA-4 therapy in upcoming research. Unfortunately, a majority of Ipilimumab treated patients still suffers from severe immune related adverse events (IRAEs). The high serum levels of Ipilimumab, resulting from systemic administration, is considered to be inherently correlated with the induction of IRAEs[10-13].

Novel concepts emerging rapidly from contemporary nanomedicine research have created interesting opportunities for the further optimization of drug delivery systems for CTLA-4 therapy. Interesting insights regarding sustained drug release and side effect management have spawned significant interests for exploring novel antibody delivery systems. Nanoparticles (NPs), polyspheres and copolymer hydrogels have for instance found a wide range of application as controlled drug delivery system in biomedical research[14-18], including also cancer research and photothermal therapy[19].

The work of Simons et al.[20] supported the notion that sustained anti-CTLA-4 release can reduce serum antibody levels. Herein a GM-CSF cell line was genetically modified to slowly release anti-CTLA-4 intracellularly, which elicited potent anti-tumor T cell responses in mice, whilst lowering serum antibody levels. Fransen et al.[21] reported that activation of local CD8 T cells with anti-CD40 antibody, provided via the slow release agent Montanide ISA-51, significantly lowered serum antibody levels. Montanide based CD40 treatment induced effective systemic CD8 T cell activation and efficient eradication of local and distant tumors. As oil (w/o emulsion) based delivery system, it however bears certain shortcomings, because injection depots cannot be resolved. Clinical studies reported that these depots can cause irritation, fever and sterile abscesses[22, 23]. Rahimian et al.[24] recently reported that local delivery of anti-CTLA-4 and anti-CD40 antibodies with polymeric microparticles (MPs) significantly reduced serum antibody levels whilst effectively suppressing tumor outgrowth.

With the promising findings of our previous studies and set-up of experimental models we have thus gained leverage for the development of a biocompatible antibody delivery system. We continue to build on the concepts of slow release using poloxamer based hydrogels. Poloxamer 407 (P407) is a biocompatible, FDA approved polymer consisting of poly(ethylene

oxide)-poly(propylene oxide)-poly(ethyelene oxide) triblock copolymers (EO-PO-EO). When dissolved in water, the polymers aggregate into micelles consisting of a hydrophobic PO core and hydrophilic EO outer shell. Increasing the temperature beyond the critical gelation temperature (CGT) induces the formation of a rigid network of micelles. This process eventually induces gelation for sufficiently concentrated P407 samples[25, 26]. The established depot then serves as slow release depot that ought to limit the systemic spread of drugs[27-29].

Injectable in situ gelling hydrogels based on poloxamer have gained significant interest in drug delivery and cancer research[30]. Researchers have for instance deployed hydrogels to optimize chemotherapeutic drug delivery. Studies showed that P407 hydrogel treatment significantly reduced systemic drug concentration and side effects, whilst efficiently mediating tumor growth inhibition[31, 32]. Studies exploring P407 hydrogels as delivery system for checkpoint antibodies are however lacking currently. To our knowledge, we are the first to deploy P407 hydrogels for the optimization of CTLA-4 therapy. We initially prepared various P407 formulations and performed physico-chemical characterizations in vitro. The human IgG antibody was exploited as model antibody to optimize in vitro and in vivo release. In vivo, effects of hydrogels on serum antibody levels and tumor growth inhibition potential were assessed. Results were contrasted with free delivery (PBS) and an oil based slow release formulation (Incomplete Freund's Adjuvant; IFA). The tissue around the injection site was furthermore examined to assess whether hydrogel injection depots can be resolved. The improved understanding and tailoring of hydrogel based drug delivery systems have significant contributions for the design of safer and more efficient immune blocking therapies.

2. Materials and methods

2.1. Preparation of hydrogel

Cold PBS (pH = 7.4) was added to the poloxamer 407 (Sigma Aldrich; Steinheim; Germany; molecular weight 9840 - 14600 g/mol) granules in a 50 mL Falcon tube and stirred for 24 h at 4 °C until all the poloxamer granules were dissolved[33]. Formulations ranging from 16 to 40% poloxamer were prepared for initial analyses. When solutions became clear, antibodies were added in the gel by mixing.

2.2. Morphology of P407 hydrogel by scanning electron microscopy (SEM)

P407 hydrogels were lyophilized and mounted on aluminum stubs and sputter coated with a platinum layer. The morphology was then observed with scanning electron microscopy (SEM; NovaSEM 450). Pore surfaces were calculated using ImageJ software.

2.3. Dynamic light scattering (DLS) measurements

DLS measurements were performed with a Malvern Zetasizer (Nano ZS, Malvern Ltd., UK). 5 and 7.5% P407 solutions were prepared and the size and poly dispersity index (PDI) of the micelles were measured at 25 °C.

2.4. Time to gelation and rheological measurements

1.5 mL Eppendorfs were kept at 20 °C or 37 °C using a water bath and 250 µL of hydrogel was pipetted up and down with 1 mL tips until the tip became clogged. The time it takes for fluidic hydrogels to reach this point is referred to as 'time to gelation'. For rheology measurements samples were measured on a Dv2T viscometer (Brookfield AMETEK) in conjunction with a CP-40 spindle. The device was controlled by RHEOCALC t (2.0.37) software. To control the temperature the measurement chamber was connected to a water bath (filled with water of approximately 5 °C), which was heated 0.1 °C per second. 500 µL of thermosensitive gel (0 degrees; stored on ice) was transferred to the measurement chamber which was cooled down to +/- 5 °C before the sample was added.

2.5. Cytotoxicity assay (MTS assay)

To assess the effects of P407 hydrogel on cell viability, D1DCs (a murine immature DC cell line; 5×10^4 cells/well)[34] and MC-38 tumor cells (5×10^3 cells/well) were cultured in 96-wells plate with titrated concentrations of P407 granules, starting at 15 mg/mL. The total volume per well was 100 µL. D1DCs cells were cultured in IMDM medium (Lonza, Walkersville, USA - #12-726F) containing Hepes (25 mM). The medium was enriched with 10% fetal calf serum (FCS; Sigma-Aldrich, St. Louis, USA), Glutamax (Gibco, Paisley, UK), ß-mercaptoethanol and 100 IU/mL penicillin/streptomycin (Gibco, Paisley, UK). 30% R1 supplement (medium containing GM-CSF) was added to complete the medium. MC-38 cells were cultured in IMDM medium (Lonza, Walkersville, USA) containing Hepes (25 mM). The medium was enriched with 10% fetal calf serum (FCS; Sigma-Aldrich, St. Louis, USA), 2 mM L-glutamine (Gibco, Paisley, UK), ß-mercaptoethanol and 100 IU/mL penicillin/streptomycin (Gibco, Paisley, UK). After 24 h, 48 h and 72 h of incubation, MTS reagent (CellTiter 96® Aqueous One, #G3581, Promega, Madison, USA) was added to the cells. Wells containing medium only were included as background measurements. Metabolic active cells convert the MTS substrate (yellow) into formazan (brown), thereby yielding an optical density (OD) that can be determined with a spectrum analyzer device. After 1 h to 4 h, depending on the conversion rate, the sample ODs were determined with a spectrum analyzer (Biolegend, Bio-Rad, iMarkset) set on 490 nm. Cell viability is expressed in percentage (%) and calculated using the following formula:

$$\%\ Cell\ viability = \frac{OD490\ nm\ treated\ cells - OD490\ nm\ background}{OD490\ nm\ untreated\ cells - OD490\ nm\ background} \times 100$$

2.6. Dendritic cell activation study

To assess the effects of P407 hydrogel granules on immune cells, D1DCs[34] were cultured in 96-well plates with increasing amounts of P407 for 48 h, up to a maximum of 15 mg/mL. Thereafter, supernatants were collected and subjected to IL-12 measurement with an IL-12p40 sandwich ELISA kit (Biolegend; San Diego; USA). D1DCs were harvested for FACS analysis. Cells were detached with PBS/EDTA (Sigma-Aldrich, St. Louis, USA), washed with FACS buffer and stained with the following antibodies: anti-CD40-APC (Biolegend; San Diego; USA - clone 3/23, #12-4612), anti-CD86-FITC (eBioscience; San Diego; USA - clone GL1, #11-0862-85) and anti-

MHC II-PE (eBioscience; San Diego; USA - clone M5/114.15.2, #12-5321-82). 7-AAD (Invitrogen, Waltham, USA - #A1310) was included for live-death cell discrimination. After 30 min staining, cells were washed with FACS buffer to remove unbound antibodies and resuspended in 100 µL FACS buffer. FACS flowcytometry was performed with a LSR-II cytometer (BD Biosciences) and data were analyzed using FlowJo (version 10).

2.7. In vitro human IgG release

Due to the relative high costs and limited availability of immune checkpoint blocking antibodies, human IgG (Nanogam ®; Sanquin Bloodbank Leiden; The Netherlands) was considered as model antibody to optimize in vitro and in vivo hydrogel release studies. To follow in vitro IgG release, the 'membrane-less method'[35, 36] as described earlier for in vitro release studies was considered. 1 mL of hydrogel mixed with 100 µg IgG was pipetted in a 15 mL falcon tube and stored at 37 °C to induce gelation. Subsequently, 4 mL of 37 °C PBS pH 7.4 was carefully layered on top of the gel layer and the tubes were placed at an orbital shaker set at 37 °C / 70 rpm. At the indicated timepoints (2 h, 4 h, 6 h, 8 h, 24 h, 48 h, 72 h, 96 h and 120 h), 1 mL sample was withdrawn and the volume was replaced with 1 mL fresh PBS. After collecting the final timepoint, IgG concentrations were determined by ELISA using protein A coating (Sigma-Aldrich, St. Louis, USA) and HRP conjugated goat-anti-human IgG (Southern Biotech, Birmingham, UK) as reported by Rahimian et al.[24].

The cumulative release was calculated according to equation (1):

$$E(\%) = \frac{V_E \sum_1^{n-1} C_i + V_0 C_n}{m_0} \times 100$$

where E(%) is the cumulative release, VE is the withdrawn volume (1 mL), V0 is the begin volume (4 mL), Ci and Cn are the IgG concentrations, i and n are the sampling times and M0 is the total amount of IgG loaded in the hydrogel (100 µg).

2.8. Mice and tumor cells

BALB/c and C57BL/6j mice were purchased from The Jackson Laboratory (USA) and housed under pathogen free conditions in the animal facilities of the Leiden University Medical Center (LUMC). The Animal Experimental Committee from the LUMC approved all experiments. CT26 murine colon carcinoma cells were cultured in IMDM medium (Lonza, Walkersville, USA) containing Hepes (25 mM). The medium was enriched with 10% fetal calf serum (FCS; Sigma-Aldrich, St. Louis, USA), 2 mM L-glutamine (Gibco, Paisley, UK), ß-mercaptoethanol and 100 IU/mL penicillin/streptomycin (Gibco, Paisley, UK). All cell lines were MAP and mycoplasma tested before the start of the experiments.

2.9. In vivo IgG release

Tumor free C57BL/6 mice were injected subcutaneously (s.c.) in the right flank with 200 µL of 75 µg human IgG, either in PBS, IFA or 25% hydrogel. IFA emulsions were prepared by dissolving

the antibodies in PBS, mixing them at 1:1 with IFA oil (DIFCO Laboratories Detroit, USA) and vortexing for 30 minutes until a homogenous w/o solution was obtained. 1 d, 2 d, 3 d and 6 d after injection, blood was drawn via tail vein cuts and centrifuged at 5000 rpm for 5 min to obtain the serum. Serum IgG levels were quantified as described in section 2.7.

2.10. Hydrogel assisted anti-CTLA-4 therapy

The efficacy of a hydrogel based CTLA-4 treatment regimen was evaluated in the CT26 colon cancer model. 10^5 CT26 cells (100 µL) were inoculated s.c. in the right flank of 6 to 8 week old BALB/c mice. 7 days after inoculation, tumors were established and the mice were treated with one shot of 50 µg anti-CTLA-4 (Syrian hamster IgG, clone 9H10; BioXCell, West Lebanon, USA) in either PBS, IFA or 25% hydrogel. Mice treated with empty hydrogels were included as negative controls. Treatments were given peri-tumorally in a volume of 200 µL. 1 d, 2 d, 3 d and 6 d after injection, blood samples were collected for anti-CTLA-4 measurements. Anti-CTLA-4 was quantified with ELISA using anti-hamster capture antibody (Southern Biotech, Birmingham, UK) and biotinylated-anti-hamster IgG (clone 192-1; BD Biosciences, New Jersey, US) as secondary antibody. Tumors were measured in three dimensions (length × width × height) and size was expressed in mm^3. The mice were sacrificed when tumor sizes exceeded 1000 mm^3 or when animals displayed signs of discomfort resulting from the tumor growth.

2.11. Statistical analysis

All data and graphs were generated and analyzed using GraphPad Prism 8.0.1 (244) software. The statistical tests performed are mentioned in the figure legends. Unless otherwise stated, data are displayed as mean ± standard deviation (SD). P values < 0.05 are regarded as statistically significant.

3. Results and discussion

3.1. P407 hydrogel thermogelling properties

P407 hydrogel time to gelation kinetics depend on temperature and P407 concentration. At 37 °C, hydrogels ideally gelate as quickly as possible to ensure proper depot formation. When gel depots are not established properly, antibodies may spread too rapidly into systemic circulation[37]. Conversely, too prompt gelation at room temperature (RT; 20 °C) is not desired as premature clogging of the injection needle should be avoided. Good injectability can be a benefit compared to formulations that require implantation[38], since it allows easy and less invasive administration of drugs. By evaluating the gelation time of differently concentrated formulations, hydrogels could thus be customized to satisfy these requirements. **Figure 1A** shows that the 16% P407 formulation could not gelate at 37 °C. Starting at 18%, gelation time was 80 s and gradually decreased to 15 s for the 40% formulation. Formulations >25%, however, bear the disadvantage of gelating rapidly at RT (180 s and 167 s for 30% and 35% formulation, respectively; **Figure 1B**) and typically have sol → gel transition temperatures (Tsol-gel) below 15 °C[26]. Tsol-gel of formulations between 20% - 25% P407 lies between 18 and 22 °C, which is in line with previous reports[39, 40]. The 25% formulation gelates gradually (297 s at RT),

thereby enabling sufficient time for injection at RT. The addition of IgG had no effect on gelation time (**Figure 1C** and **D**). To visualize the sol → gel transition, 2 mL of 25% hydrogel was added in a glass bottle and held at different angles. Hydrogels appear as a fluid below the critical gelation temperature (CTC) of 18 °C and flow freely by inverting the glass bottle as shown in the upper panels of **Figure 1E**. At this stage the gel flows freely in the syringe and can be injected smoothly. As such, hydrophilic compounds can be easily incorporated in the hydrogel by simple mixing (shown here with Trypan blue). When rising the temperature beyond this CGT, gelation is induced and a semi solid mass is formed that will not flow upon inversion of the glass bottle. The gelation process is reversible by decreasing the temperature to below 18 °C. In **Figure 1F** rheological measurements (gelation kinetics) of 25% P407 hydrogels are shown. Viscosity, displayed as cP, increased upon temperature increase, but IgG did not affect hydrogel gelation kinetics. Regarding the good injectability, quick gelation at 37 °C and ease of IgG incorporation, the 25% P407 formulation was subjected to subsequent analysis. FTIR and NMR analysis (**Supplementary Figure S1**) were comparable with data that is available in literature[41-43], suggesting that the material was free from impurities.

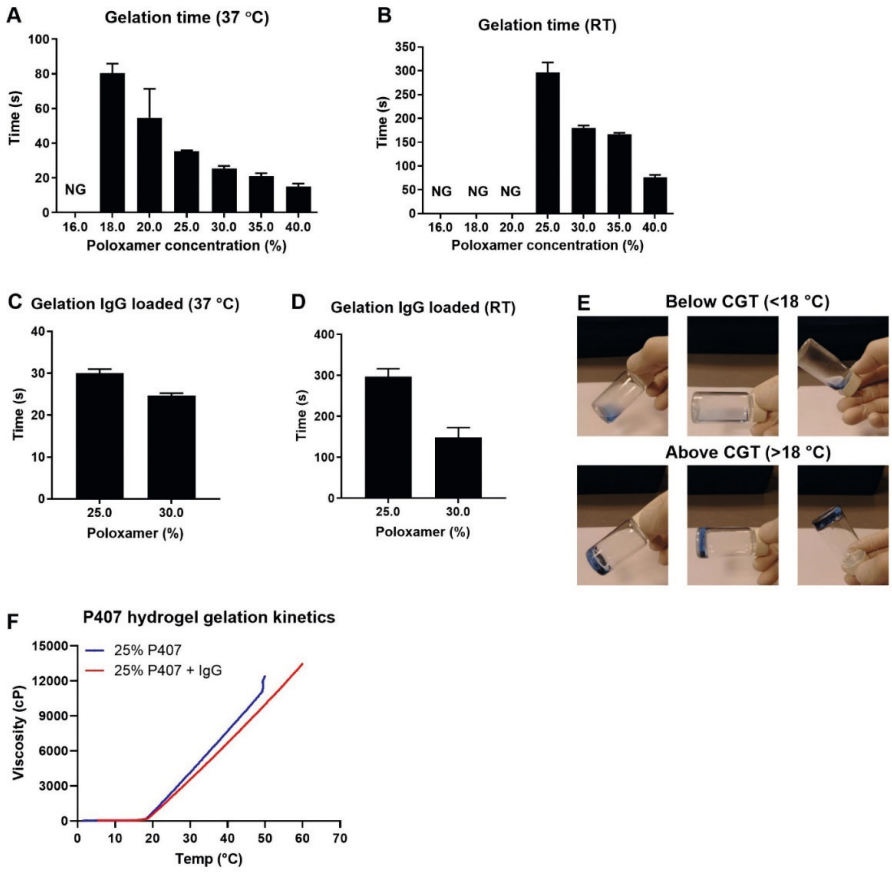

Figure 1. Time to gelation at 37 °C (A) and RT (B) was measured by pipetting hydrogels of varying concentrations up and down until the tip became clogged. NG: no gelation. Time to gelation data for IgG loaded hydrogels (25 and 30%) are depicted in (C) and (D). Results are shown as mean ± SD for a triplicate measurement. Photographical images (E) display sol-to-gel transition for the 25% hydrogel formulation. Trypan blue was added to visualize the gel. CGT: critical gelation temperature. Rheological measurements (F) were performed to assess the gelation kinetics of 25% P407 hydrogels.

3.2. Hydrogel SEM microscopy and dynamic light scattering measurements

SEM microscopy revealed the abundant porous structure of the 25% P407 hydrogel at various magnifications (**Figure 2**). The 500× and 1000× (**Figure 2B** and **C**) magnifications represent zoom-ins of representative areas from the 100× magnification (**Figure 2A**). As is notably evident from the 500× and 1000× magnifications, the pores have round and oval shapes, with an average pore surface of 1335 ± 203 μm^2 (quantified by ImageJ). This porous, channel-like structure results from the ordered packaging of micelles upon temperature increase and gelation. Micelles already start to form at 5 to 7.5% P407 concentration. In **Figure 2D**, a representative size distribution histogram of the micelle solution is shown, with the smaller peak at 5 nm representing the size of a individual micelle and the larger peak the aggregation

of micelles. At 5% solution the average size was 28.22 nm with a PDI of 0.31 (**Figure 2E**). For the 7.5% solution, average size was 28.04 nm with a PDI of 0.37 (**Figure 2F**).

This resulting porous structure is supposed to drive the diffusion of hydrophilic compounds such as antibodies. On the other hand, pores promote the breakdown of hydrogels upon exposure to aqueous media[44]. Considering the fact that IgG and anti-CTLA-4 antibodies have an average size of 13.5 nm[45], with a molar mass of 150.000 g/mol, antibodies should diffuse unhindered through the channels.

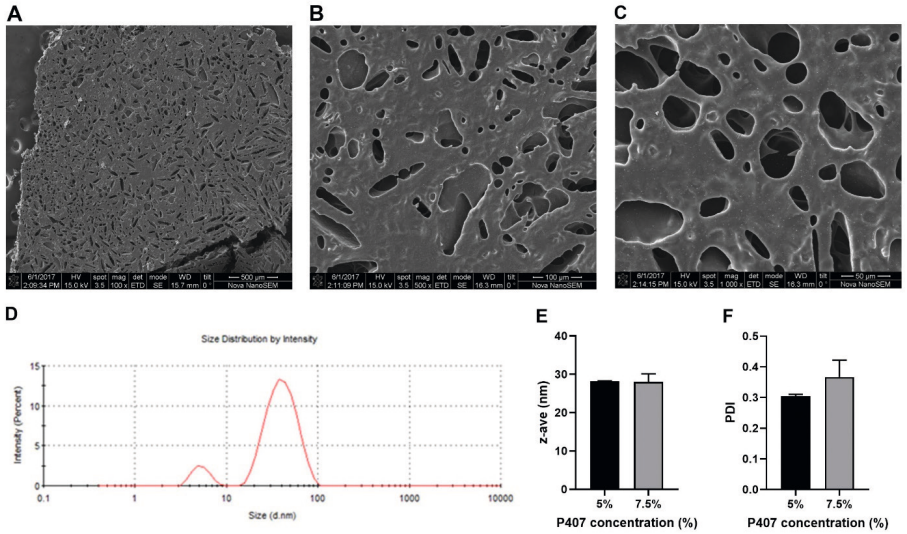

Figure 2. SEM images reveal the porous structure of 25% P407 hydrogel at 100× (A), 500× (B) and 1000× (C) magnification. A representative histogram for the micelle size is depicted in (D; left peak at 5 nm) and the average size (z-ave) and PDI are depicted in (E) and (F), respectively. Results are shown as mean ± SD for a triplicate measurement.

3.3. 25% P407 hydrogel promotes sustained IgG release

Human IgG antibody (Nanogam ®) was deployed as representative model antibody to mimic and optimize the release of immunomodulatory antibodies. 1 mL of fluidic 25% hydrogel was pipetted in an Eppendorf and IgG antibody was incorporated by just simply mixing with the gel at RT. As such, antibodies were easily incorporated in the hydrogel and no antibodies were lost during hydrogel preparation. After gelation was induced by putting the gel at 37 °C, PBS pH 7.4 was layered on top, which served as release medium. At regular intervals, release medium was withdrawn for IgG measurement. The release study (**Figure 3**) demonstrates that the hydrogel shows low initial burst release, with 50% of the loaded amount of IgG being released within approximately 48 h. Peak burst release shortly after injection is not desired as this leads to high systemic concentration antibodies, which could consequently trigger immune side effects[46]. After 120 h, hydrogels were completely resolved and it was indeed evident that no antibodies were lost during hydrogel preparation, since the entire IgG load of 100 µg was

retrieved. This has great economic advantages, because this limits the need for loading extra amounts of antibodies. Considering the low initial burst release as well as the sustained release up to 120 h, it could be envisaged that in vitro antibody kinetics were favorable. Regarding the hydrophilicity of IgG, the porous structure of P407 as well as its erosion upon exposure to water[47, 48], it is conceivable that both hydrogel breakdown as well as diffusion are driving IgG release.

There are studies reporting a quicker release time (48 h) with P407 gels but release can be ascribed to differences in the experimental approach[31, 32, 49]. In these studies, the entire release medium volume was taken out and replaced with an equal volume of fresh medium. This method can cause quicker hydrogel erosion, which consequently results in quicker drug release. We considered protocols where a smaller fraction of the release volume is refreshed[50, 51]. Release was completed when no hydrogel layer could be observed, which was after 120 h.

Though the release kinetics shown here appears satisfying, for certain (immuno)therapies a longer release rate might be desired. For P407 hydrogels, crosslinkers are typically considered to strengthen gels and improve release kinetics. For example, ß-glycerolphosphate has already been proposed for the crosslinking of chitosan-P407 hydrogels to improve its stability and release kinetics. For checkpoint blocking immunotherapy, the use of crosslinking agents must however be scrutinized carefully, since chitosan (and its derivatives) has been reported to be immunogenic or even exert cytotoxic effects. Moreover, high concentration crosslinkers may be necessary, which could substantially compromise biocompatibility and injectability[52, 53].

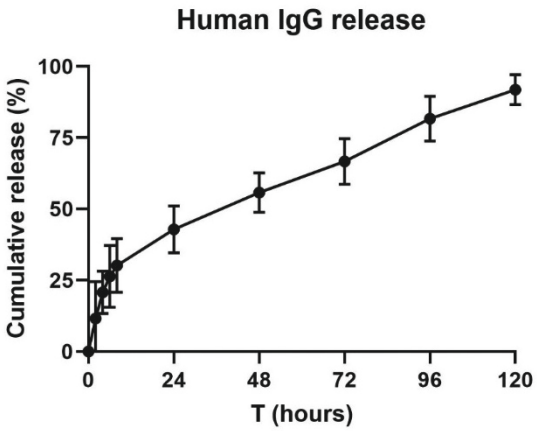

Figure 3. In vitro human IgG release from 25% P407 hydrogel. Hydrogels loaded with 100 µg IgG were loaded in 15 mL Falcon tubes and 37 °C PBS pH 7.4 was layered on top to serve as release medium. At the indicated time-points, release medium was collected and IgG levels were quantified with ELISA. Results are shown as mean ± SD for two independent experiments, with N = 6 in total.

3.4. P407 hydrogel does not exert cytotoxicity in vitro

It is crucial to ensure that the P407 hydrogel is well-tolerated. To this end, we tested P407 on two cell lines. D1DCs (an immature murine dendritic cell line) and MC-38 (murine colon cancer) cells were incubated with titrated doses of P407 and cell viability was assessed with MTS. As is evident from **Figure 4**, cell viability in D1 cells (**A – C**) as well as MC-38 cells (**D – F**) did not decrease over time for any concentrations up to 15 mg/mL. Our data indicate that P407 is biocompatible and does not exert tumoricidal effects by itself. This corroborates data from previous research, where for instance is shown that poloxamer hydrogel is a biocompatible encapsulation material for (stem) cells[54-56].

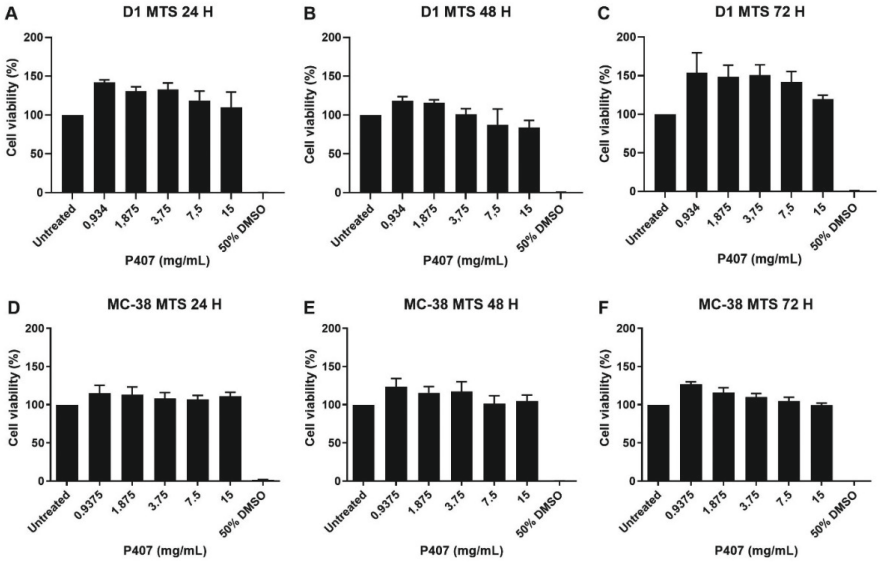

Figure 4. P407 exerts no cytotoxic effects on D1DCs and MC-38 cells. D1DCs (A – C) and MC-38 cells (D – F) were incubated for 24 h, 48 h and 72 h with increasing concentrations of P407 up to a maximum of 15 mg/mL. 50% DMSO in medium served as positive control. After incubation, MTS reagent was added and the change of optical density of the formed product was measured at 490 nm. Data are shown as mean ± SD for a triplicate measurement.

3.5. P407 hydrogel does not activate TLR signaling pathways in D1DCs

An undesired effect of biopolymer based drug carriers could be immunogenicity[57]. Although it has been reported that a combination of P407 and chitosan exerts immune-modulatory effects in vitro[58], the effect of P407 on immune cells responsible for eliciting anti-tumor immunity remains obscure. It is thus crucial to discern between the effects the drug carrier may exert and the actual effects conferred by the encapsulated immunotherapeutic antibodies. To address this, we assessed whether P407 activates signaling pathways in dendritic cells. D1DCs elevate the expression of co-stimulatory markers upon encountering various danger or toxic signals, amongst others from Toll-like receptor ligands (TLR-L)[59-61]. The associated

pathways stay central to the propagation of CTL T cell priming and evoking of anti-tumor immunity. Therefore, D1DCs were incubated with titrated concentrations of P407. After 48 h, expression of the co-stimulatory markers CD86, CD40 and MHC-II and production of the pro-inflammatory cytokine IL-12 were evaluated. For FACS flowcytometry, doublet cells were gated out and analysis was performed in the 7-AAD negative population (**Figure 5A**). As shown in **Figure 5B**, P407 concentrations up to 15 mg/mL did not induce CD86, MHC-II and CD40 expression, as opposed to D1DCs treated with the TLR-3L poly (I:C)(**Figure 5C**). Consistent with these findings, P407 did not induce IL-12 production at any concentration (**Figure 5D**), as opposed to poly (I:C)(**Figure 5E**). In conclusion, these data suggest that P407 does not induce immune activation. This is an important property since it indicates that hydrogels are inert and do not trigger immune activation by themselves. Furthermore, these results indicate that the hydrogels were sterile and absent of pathogens or endotoxins.

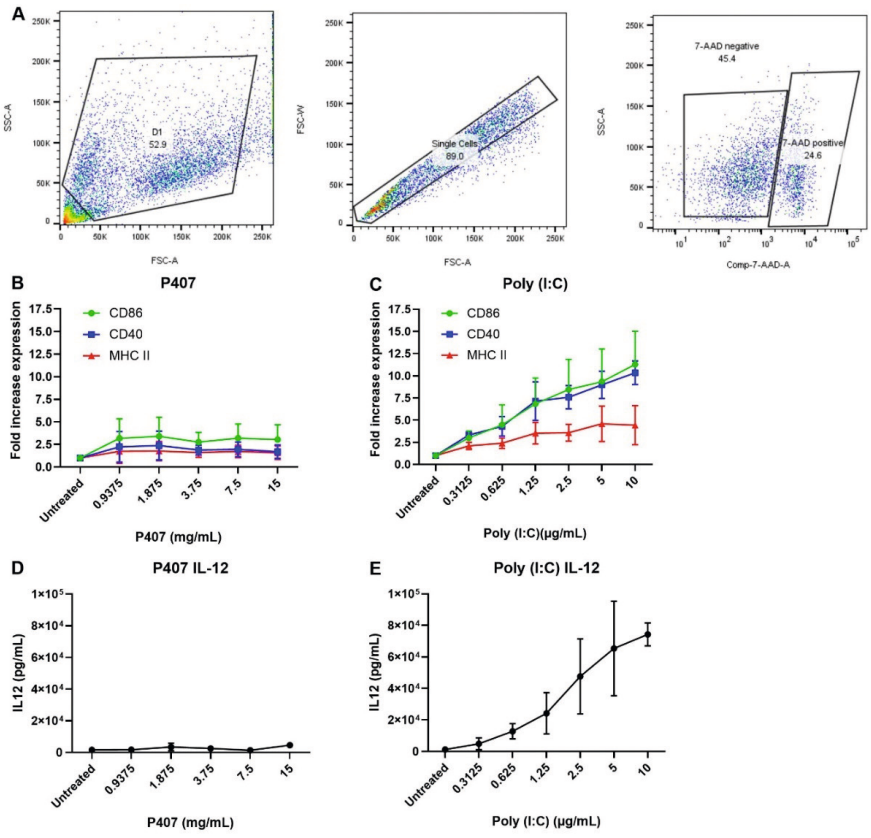

Figure 5. In vitro D1DC activation measured with FACS flowcytometry and IL-12 ELISA. D1DCs were incubated with increasing concentrations of P407 for 48 h. Poly (I:C) served as positive control. Gating strategy is shown in (A) and analysis was performed on the 7-AAD negative population. The differences in CD86, MHC-II and CD40 expression are shown as fold change expression (compared to untreated; B and C). IL-12 production (D and E) is shown in pg/mL. Data is shown as mean ± SD for three independent experiments.

3.6. Injectable hydrogel formulations reduce serum IgG levels and injection depots are cleared in vivo

To evaluate the effects of hydrogel mediated antibody delivery on serum antibody levels, hydrogels incorporated with 75 µg of human IgG antibody were injected s.c. in C57BL/6 mice. During treatment hydrogels remained fluidic, which easily facilitated the injection. At the indicated time-points, blood was sampled to quantify serum IgG levels. As shown in **Figure 6A**, IgG delivery via PBS induced high peak levels of antibody notably within the first three days (peaking at day 1). In stark contrast, hydrogel IgG delivery significantly lowered serum antibody levels; IgG levels were comparable with that of IFA treated mice (**Figure 6A**). Early analyses revealed that differences between PBS and hydrogel delivery were most apparent within the first 24 h after injection. Consistent with the in vitro release data, hydrogels induced minimal burst release within the first 6 h (**Supplementary Figure S2**). Hydrogel treated mice neither displayed weight loss nor other signs of discomfort (**Figure 6B**), suggesting that the hydrogels were well-tolerated. Shortly after injection, gel depots were clearly established (**Figure 6C**, appearance after sacrificing), but were clearly resolved within 14 d after injection (**Figure 6D**). This observation is consistent with the degradation rate in vitro, where gels were fully degraded after 5 days. Altogether, these observations support previous studies showing that poloxamer is biocompatible and that gel depots can be resolved in vivo[62-64]. This represents a clear advantage over oil based slow release formulations such as IFA and Montanide. Depots from these formulations cannot be resolved after injection and can induce swelling, pain and inflammation (**Figure 6E**)[65, 66]. A study by Mao et al.[51] reported that P407 does not induce inflammation in vivo, as determined by histological analysis. Taken together, hydrogels reduce serum IgG levels, are biocompatible and depots can be resolved, measures which are indicative for the reduction of side effects.

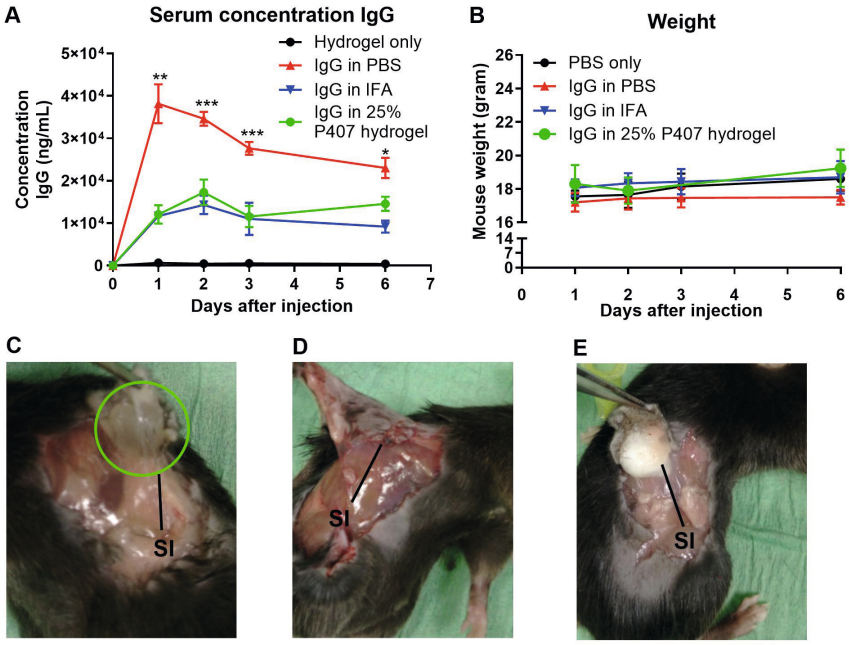

Figure 6. Serum IgG antibody levels following s.c. injection of 25% P407 hydrogel incorporated with 75 µg IgG. (A) Tail vein blood was drawn at the indicated time-points and serum IgG levels were measured with ELISA, with statistical differences being assessed using an unpaired Student's T Test (* $P<0.05$, ** $P<0.01$, *** $P<0.001$). (B) Body weight follow-up during treatment period. Data are shown as mean ± SD with N = 3 mice per group. (C) Appearance of P407 hydrogel depot formed under the skin 5 min after injection. (D, E) Post-mortal analysis of the skin at the site of injection (SI) 14 days after P407 hydrogel (D) or IFA (E) treatment.

3.7. P407 hydrogel anti-CTLA-4 delivery reduces serum antibody levels and facilitates effective tumor growth inhibition in CT26 tumor model

The efficacy of hydrogel based CTLA-4 therapy to inhibit tumor growth was assessed in the CT26 model. 7 days after inoculation, mice received empty hydrogel treatment or one shot of 50 µg of anti-CTLA-4 in PBS, IFA or 25% P407 hydrogel. At the indicated moments, blood was drawn for measuring serum anti-CTLA-4 levels (**Figure 7A**). **Figure 7B** shows that empty hydrogel treatment alone did not slow down tumor outgrowth. In a one-by-one comparison, it was clear that hydrogels neither slowed down, nor accelerated tumor growth (**Supplementary Figure S3**). This indicates that P407 hydrogels were inert and do not interfere with the CTLA-4 therapy. It is essential to ensure that drug delivery systems do not cause adverse effects. Fransen et al.[67] for instance evaluated dextran-based MPs as slow release system for CD40 immunotherapy. Whilst MPs indeed reduced systemic side effects, unfortunately MPs were reported to induce inflammation that was associated with rapid tumor outgrowth. Mice treated with anti-CTLA-4 in hydrogel showed significant delay of tumor outgrowth to a comparable extent as the groups receiving CTLA-4 treatment in PBS and IFA. The survival curves (**Figure**

7C) show that hydrogel CTLA-4 treatment significantly improved survival compared to mice receiving the hydrogel mock treatment. Survival was comparable with CTLA-4 treatment in PBS and IFA. From these results, it is evident that antibodies released from hydrogels maintain their functional activity. Consistent with a binding assay using anti-PD-L1 antibody, we found that the incorporation of anti-PD-L1 antibody in hydrogels did not affect its binding efficacy to PD-L1 receptor (**Supplementary Figure S4**).

Serum anti-CTLA-4 levels raised rapidly in mice treated with anti-CTLA-4 in PBS. In contrast, mice receiving hydrogel + anti-CTLA-4 displayed a significant reduction of serum anti-CTLA-4 levels (**Figure 7D**). A limitation with the release study is that it only detects the anti-CTLA-4 levels in circulation. It remains to be explored for example why antibody levels were dropping after 6 h; antibodies might have been cleared or sequestered to their target cells and tissues. Further studies dedicated to these questions can be useful to find out where antibodies might end up on long term period. The photograph in **Figure 7E** is showing a post-mortal analysis of a hydrogel (left) and IFA (right) treated mouse, which were both sacrificed 20 d post treatment due to tumor burden. Consistent with the images obtained during the in vivo hydrogel IgG release, these images clearly show that hydrogel depots were fully resolved whereas IFA depots could not be cleared. In another tumor model (MC-38 colon cancer) hydrogel mediated CTLA-4 blockade resulted in a comparable extent of tumor growth inhibition as in the CT26 model (**Supplementary Figure S5**). Altogether, poloxamer hydrogels represent promising platforms for CTLA-4 blockade by means of reduction of systemic antibody levels, biocompatibility and facilitating effective tumor growth inhibition. Hydrogels injection depots were moreover clearly resolved after 1 week of treatment.

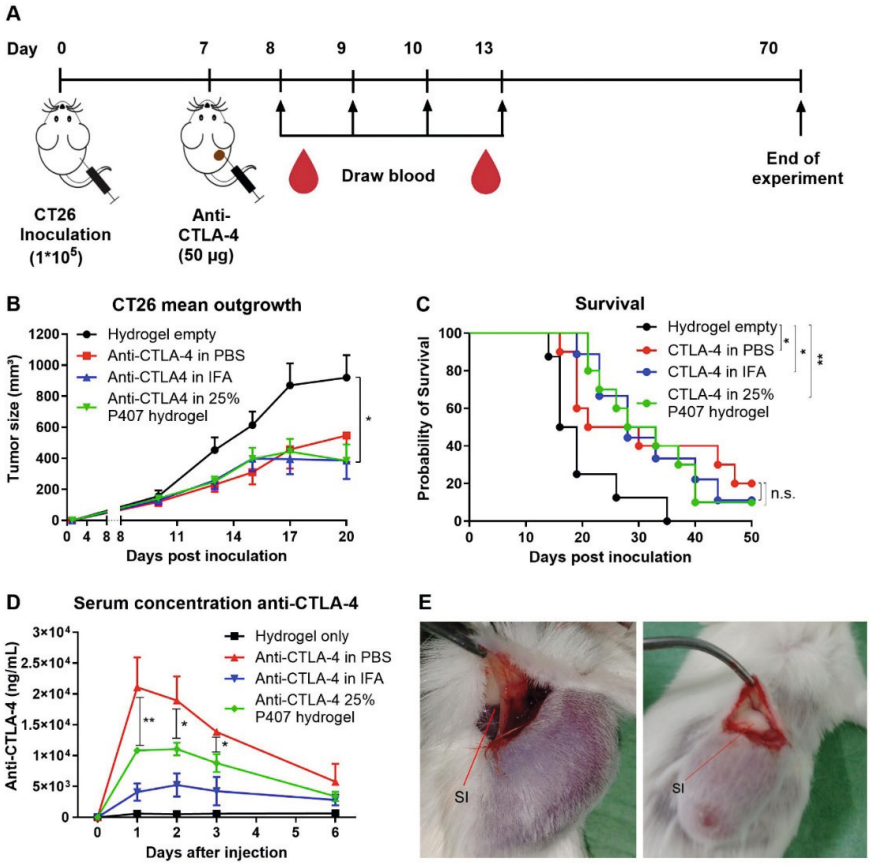

Figure 7. P407 hydrogel based CTLA-4 blockade in CT26 model. The experimental procedures are depicted chronologically in (A). Average tumor outgrowth curves of CT26 tumor bearing mice after treatment with empty hydrogel (N=8), anti-CTLA-4 in PBS (free; N=10), IFA (N=10) or 25% hydrogel (N=10) are shown in (B) with the associated survival curves in (C). In (D) the serum anti-CTLA-4 levels for the different treatments are depicted (N=3). Post-mortal analysis (E) was performed to inspect the skin area at the site of injection (SI) for animals injected with hydrogel (left) or IFA (right). Differences in average tumor size were assessed with a Mann-Whitney U test. Differences in serum antibody levels were assessed with an unpaired Student's T test and survival analysis was performed with a Log-rank test, with * $p<0.05$ and ** $p<0.01$. Representative data of two experiments are shown. N.S.: not significant

4. Conclusions

In conclusion, P407 hydrogels are potentially promising delivery systems to improve CTLA-4 immunotherapy supported by the following notions. P407 hydrogels were easily injectable, thereby allowing a minimally invasive treatment procedure. Antibodies were easily added in the gel by mixing and no antibodies were lost during preparation. In vivo, hydrogels reduced serum antibody levels comparable to IFA without inducing cytotoxicity. In contrast to IFA, hydrogels

were biocompatible and injection depots were clearly resolved. Finally, we demonstrated that hydrogel based CTLA-4 therapy effectively mediated tumor growth inhibition.

These results make important contributions in the field of cancer immunotherapy. CTLA-4 therapy is potential cancer treatment modality, but its therapeutic utility can be limited owing to uncontrolled antibody spread and induction of severe side effects. Biocompatible release platforms that can control antibody release are therefore gaining interest in cancer immunotherapy research. It is conceivable that future studies will optimize P407 hydrogels as delivery systems for other checkpoint antibodies, such as PD-1, anti-PD-L1 or a combination of them. Furthermore, hydrogels may gain interest for the delivery of immune adjuvants or cancer vaccination compounds, to control for instance the release of antigens and thereby sustain immune activation[68]. The combinations of molecules that can be included in the hydrogel – with regard to solubility for instance – however still requires extensive research which is necessary to expand the utility of hydrogel drug delivery systems. Altogether, hydrogel delivery systems create promising new avenues of research for the optimization of cancer immunotherapies.

Data availability

The authors declare that all data supporting this study are available within the manuscript or can be obtained from the authors upon request.

Appendix: Supplementary data

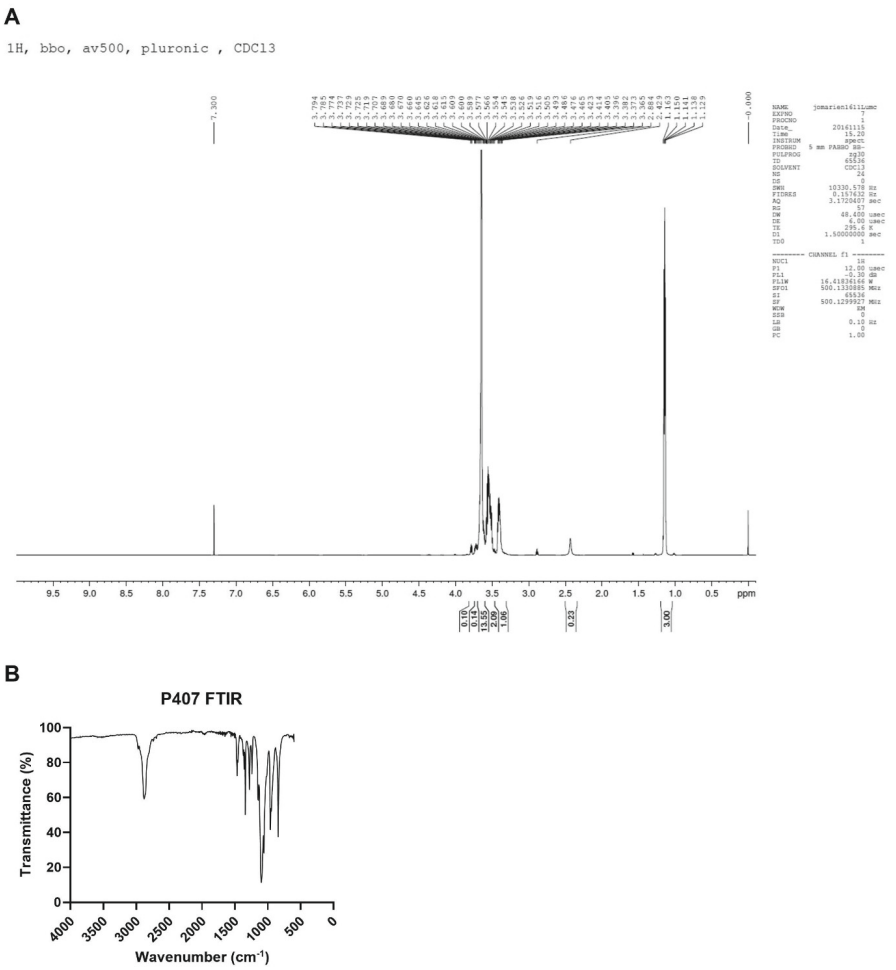

Figure S1. H-NMR and FTIR measurements of P407. H-NMR measurements (A) were taken with AVANCE 600 spectrometer (Bruker, Germany). FTIR (B) spectra were obtained using a Bruker spectrometer (Bruker, Germany) within the wavenumber range from 4000 to 500 cm^{-1}.

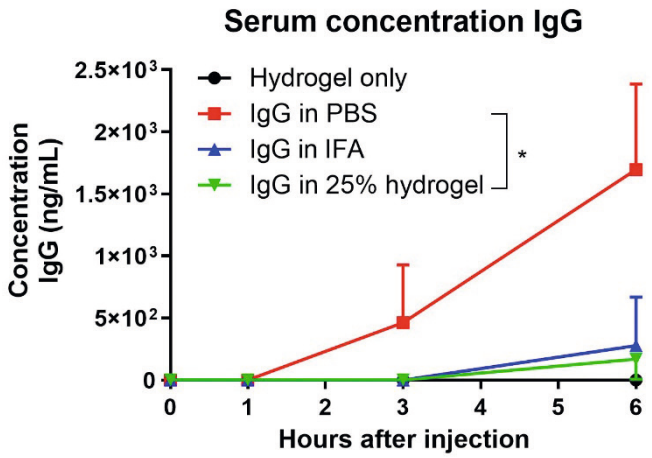

Figure S2. Serum IgG levels differences are most pronounced within the first 6 h. Mice received either IgG in PBS, IFA or 25% hydrogel and blood was drawn 0, 1, 3 and 6 h following treatment. Data is shown as mean ± SD with N = 3.

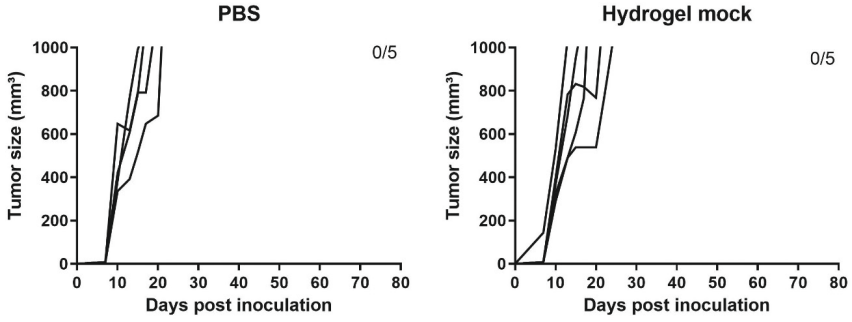

Figure S3. Hydrogel mock treatment exerts no effect on CT26 tumor growth. The graphs depict tumor outgrowth (mm^3) for PBS (left) and hydrogel mock (right) treated mice.

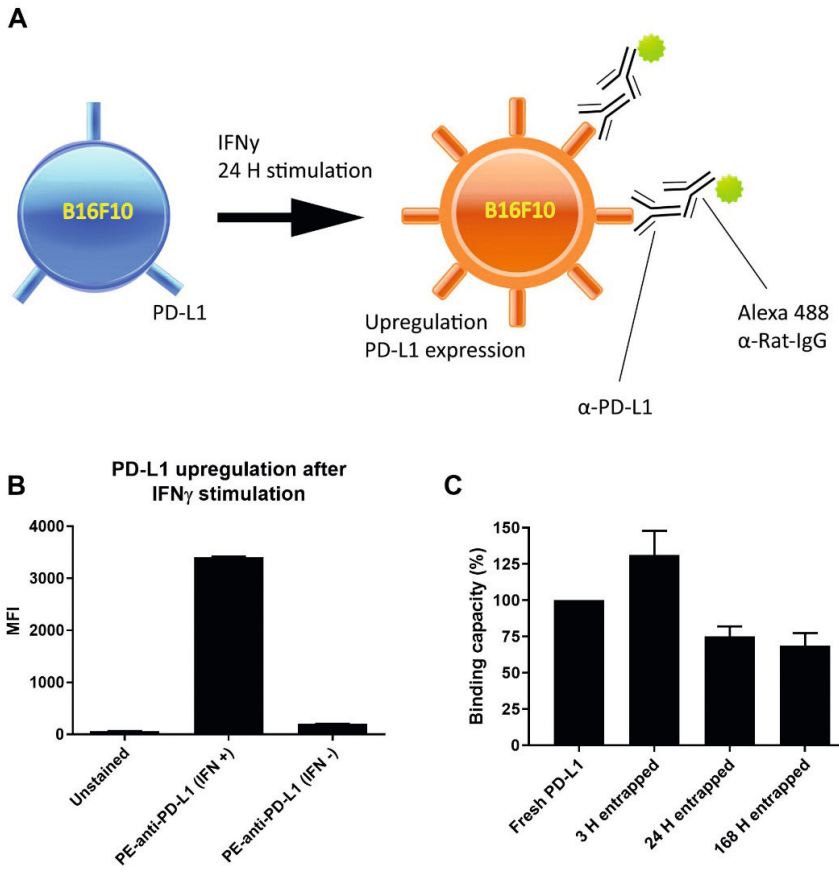

Figure S4. Evaluating binding capacity of anti-PD-L1 after entrapment in hydrogel. 50 µg of anti-PD-L1 was entrapped in 300 µL 25% P407 hydrogels for 3, 24 and 168 h. Gelation was induced upon placement of the samples at 37 °C. After the indicated timepoints, samples were put at 4 °C to reverse the gelling process, in order to liberate all the antibodies that were still entrapped in the gel. (A) Schematic representation of experimental set-up. B16F10 cells were incubated 24 h with 10 IU/mL to upregulate PD-L1 expression (B). Thereafter cells were harvested, washed and incubated with the anti-PD-L1 that has been liberated from the gels. In the subsequent step, cells were stained with fluorescent labelled anti-rat IgG (Alexa 488 donkey-anti-rat IgG). Alexa 488 fluorescence – as a measure of PD-L1 binding – was compared to that of PD-L1 that came freshly out of the stock ('fresh PD-L1'). Data was finally normalized to 'fresh PD-L1' and depicted as % binding capacity (C). Data is shown as mean ± SD with N = 3.

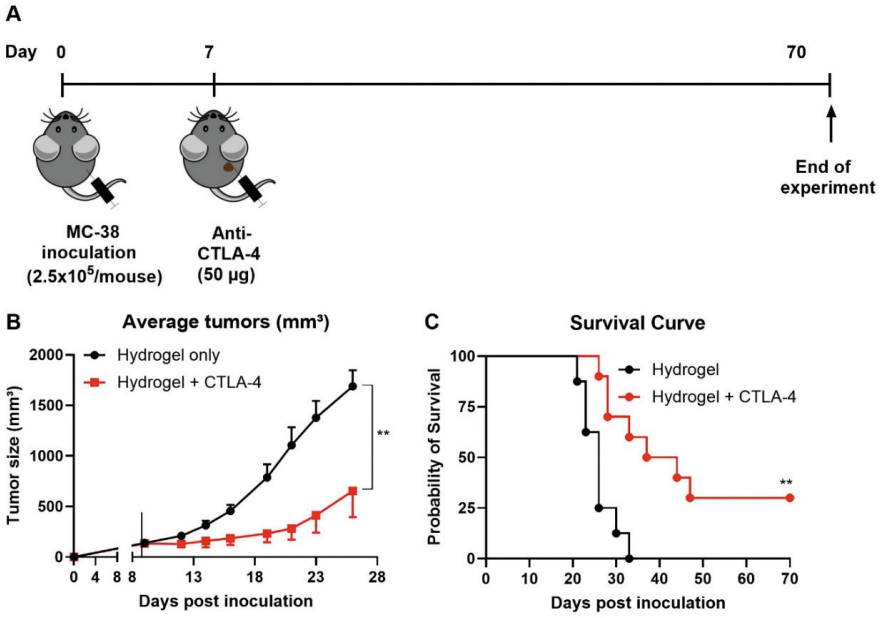

Figure S5. Hydrogel CTLA-4 treatment confers tumor growth inhibition in MC-38 colon cancer. The experimental procedure is depicted chronologically in (A). Mice were inoculated with 2.5×10^5 MC-38 cells and 7 days later mice received one shot of 50 µg anti-CTLA-4 peri-tumorally. Average tumor outgrowth curves of MC-38 tumor bearing mice after treatment with empty hydrogel or anti-CTLA-4 in hydrogel (both N=10) are shown in (B), with the associated survival curves shown in (C). Differences in average tumor growth were assessed with a Mann-Whitney U test and survival was analyzed by a Log-rank test, with ** $p<0.01$.

5. References

1. Y.J. Park, D.S. Kuen, Y. Chung, Future prospects of immune checkpoint blockade in cancer: from response prediction to overcoming resistance, Exp Mol Med. 50 (2018) 109.
2. P. Letendre, V. Monga, M. Milhem, Y. Zakharia, Ipilimumab: from preclinical development to future clinical perspectives in melanoma, Future Oncol. 13 (2017) 625-636.
3. D.M. Pardoll, The blockade of immune checkpoints in cancer immunotherapy, Nature reviews. Cancer. 12 (2012) 252-264.
4. J.A. Seidel, A. Otsuka, K. Kabashima, Anti-PD-1 and Anti-CTLA-4 Therapies in Cancer: Mechanisms of Action, Efficacy, and Limitations, Front Oncol. 8 (2018) 86.
5. M.L. Alegre, K.A. Frauwirth, C.B. Thompson, T-cell regulation by CD28 and CTLA-4, Nat Rev Immunol. 1 (2001) 220-228.
6. F.S. Hodi, S.J. O'Day, D.F. McDermott, R.W. Weber, J.A. Sosman, J.B. Haanen, et al., Improved survival with ipilimumab in patients with metastatic melanoma, The New England journal of medicine. 363 (2010) 711-723.
7. D. McDermott, J. Haanen, T.T. Chen, P. Lorigan, S. O'Day, M.D.X. Investigators, Efficacy and safety of ipilimumab in metastatic melanoma patients surviving more than 2 years following treatment in a phase III trial (MDX010-20), Ann Oncol. 24 (2013) 2694-2698.
8. D. Schadendorf, F.S. Hodi, C. Robert, J.S. Weber, K. Margolin, O. Hamid, et al., Pooled Analysis of Long-Term Survival Data From Phase II and Phase III Trials of Ipilimumab in Unresectable or Metastatic Melanoma, Journal of clinical oncology : official journal of the American Society of Clinical Oncology. 33 (2015) 1889-1894.
9. P.A. Ascierto, M. Del Vecchio, C. Robert, A. Mackiewicz, V. Chiarion-Sileni, A. Arance, et al., Ipilimumab 10 mg/kg versus ipilimumab 3 mg/kg in patients with unresectable or metastatic melanoma: a randomised, double-blind, multicentre, phase 3 trial, Lancet Oncol. 18 (2017) 611-622.
10. C.J. Voskens, S.M. Goldinger, C. Loquai, C. Robert, K.C. Kaehler, C. Berking, et al., The price of tumor control: an analysis of rare side effects of anti-CTLA-4 therapy in metastatic melanoma from the ipilimumab network, PloS one. 8 (2013) e53745.
11. C.F. Friedman, T.A. Proverbs-Singh, M.A. Postow, Treatment of the Immune-Related Adverse Effects of Immune Checkpoint Inhibitors: A Review, JAMA Oncol. 2 (2016) 1346-1353.
12. P. Attia, G.Q. Phan, A.V. Maker, M.R. Robinson, M.M. Quezado, J.C. Yang, et al., Autoimmunity correlates with tumor regression in patients with metastatic melanoma treated with anti-cytotoxic T-lymphocyte antigen-4, Journal of clinical oncology : official journal of the American Society of Clinical Oncology. 23 (2005) 6043-6053.
13. J.M. Michot, C. Bigenwald, S. Champiat, M. Collins, F. Carbonnel, S. Postel-Vinay, et al., Immune-related adverse events with immune checkpoint blockade: a comprehensive review, Eur J Cancer. 54 (2016) 139-148.
14. R. Boppana, S. Yadaorao Raut, G. Krishna Mohan, B. Sa, S. Mutalik, K.R. Reddy, et al., Novel pH-sensitive interpenetrated network polyspheres of polyacrylamide-g-locust bean gum and sodium alginate for intestinal targeting of ketoprofen: In vitro and in vivo evaluation, Colloids and Surfaces B: Biointerfaces. 180 (2019) 362-370.
15. V. Dave, K. Tak, A. Sohgaura, A. Gupta, V. Sadhu, K.R. Reddy, Lipid-polymer hybrid nanoparticles: Synthesis strategies and biomedical applications, Journal of Microbiological Methods. 160 (2019) 130-142.
16. V. Dave, A. Gupta, P. Singh, C. Gupta, V. Sadhu, K.R. Reddy, Synthesis and characterization of celecoxib loaded PEGylated liposome nanoparticles for biomedical applications, Nano-Structures & Nano-Objects. 18 (2019) 100288.

17. S. Gulla, D. Lomada, V.V.S.S. Srikanth, M.V. Shankar, K.R. Reddy, S. Soni, et al., Chapter 11 - Recent advances in nanoparticles-based strategies for cancer therapeutics and antibacterial applications, in: V. Gurtler, A.S. Ball, S. Soni (Eds.) Methods in Microbiology, Academic Press, 2019, pp. 255-293.
18. S.B. Patil, S.Z. Inamdar, K.K. Das, K.G. Akamanchi, A.V. Patil, A.C. Inamadar, et al., Tailor-made electrically-responsive poly(acrylamide)-graft-pullulan copolymer based transdermal drug delivery systems: Synthesis, characterization, in-vitro and ex-vivo evaluation, Journal of Drug Delivery Science and Technology. 56 (2020) 101525.
19. N. Xia, N. Li, W. Rao, J. Yu, Q. Wu, L. Tan, et al., Multifunctional and flexible ZrO2-coated EGaIn nanoparticles for photothermal therapy, Nanoscale. 11 (2019) 10183-10189.
20. A.D. Simmons, M. Moskalenko, J. Creson, J. Fang, S. Yi, M.J. VanRoey, et al., Local secretion of anti-CTLA-4 enhances the therapeutic efficacy of a cancer immunotherapy with reduced evidence of systemic autoimmunity, Cancer immunology, immunotherapy : CII. 57 (2008) 1263-1270.
21. M.F. Fransen, M. Sluijter, H. Morreau, R. Arens, C.J. Melief, Local activation of CD8 T cells and systemic tumor eradication without toxicity via slow release and local delivery of agonistic CD40 antibody, Clinical cancer research : an official journal of the American Association for Cancer Research. 17 (2011) 2270-2280.
22. B.S. Graham, M.J. McElrath, M.C. Keefer, K. Rybczyk, D. Berger, K.J. Weinhold, et al., Immunization with cocktail of HIV-derived peptides in montanide ISA-51 is immunogenic, but causes sterile abscesses and unacceptable reactogenicity, PloS one. 5 (2010) e11995.
23. C.R. Alving, Design and selection of vaccine adjuvants: animal models and human trials, Vaccine. 20 Suppl 3 (2002) S56-64.
24. S. Rahimian, M.F. Fransen, J.W. Kleinovink, M. Amidi, F. Ossendorp, W.E. Hennink, Polymeric microparticles for sustained and local delivery of antiCD40 and antiCTLA-4 in immunotherapy of cancer, Biomaterials. 61 (2015) 33-40.
25. M.S. Akash, K. Rehman, Recent progress in biomedical applications of Pluronic (PF127): Pharmaceutical perspectives, Journal of controlled release : official journal of the Controlled Release Society. 209 (2015) 120-138.
26. G. Dumortier, J.L. Grossiord, F. Agnely, J.C. Chaumeil, A review of poloxamer 407 pharmaceutical and pharmacological characteristics, Pharm Res. 23 (2006) 2709-2728.
27. M.M. Amiji, P.K. Lai, D.B. Shenoy, M. Rao, Intratumoral administration of paclitaxel in an in situ gelling poloxamer 407 formulation, Pharm Dev Technol. 7 (2002) 195-202.
28. C. Ju, J. Sun, P. Zi, X. Jin, C. Zhang, Thermosensitive micelles-hydrogel hybrid system based on poloxamer 407 for localized delivery of paclitaxel, J Pharm Sci. 102 (2013) 2707-2717.
29. Z. Wei, J. Hao, S. Yuan, Y. Li, W. Juan, X. Sha, et al., Paclitaxel-loaded Pluronic P123/F127 mixed polymeric micelles: formulation, optimization and in vitro characterization, Int J Pharm. 376 (2009) 176-185.
30. M. Sharma, A. Deohra, K.R. Reddy, V. Sadhu, Chapter 5 - Biocompatible in-situ gelling polymer hydrogels for treating ocular infection, in: V. Gurtler, A.S. Ball, S. Soni (Eds.) Methods in Microbiology, Academic Press, 2019, pp. 93-114.
31. S. Nie, W.L. Hsiao, W. Pan, Z. Yang, Thermoreversible Pluronic F127-based hydrogel containing liposomes for the controlled delivery of paclitaxel: in vitro drug release, cell cytotoxicity, and uptake studies, Int J Nanomedicine. 6 (2011) 151-166.
32. J.J. Xuan, Y.D. Yan, D.H. Oh, Y.K. Choi, C.S. Yong, H.G. Choi, Development of thermo-sensitive injectable hydrogel with sustained release of doxorubicin: rheological characterization and in vivo evaluation in rats, Drug Deliv. 18 (2011) 305-311.
33. T. Gratieri, G.M. Gelfuso, E.M. Rocha, V.H. Sarmento, O. de Freitas, R.F. Lopez, A poloxamer/chitosan in situ forming gel with prolonged retention time for ocular delivery, Eur J Pharm Biopharm. 75 (2010) 186-193.

34. D.H. Schuurhuis, S. Laban, R.E. Toes, P. Ricciardi-Castagnoli, M.J. Kleijmeer, E.I. van der Voort, et al., Immature dendritic cells acquire CD8(+) cytotoxic T lymphocyte priming capacity upon activation by T helper cell-independent or -dependent stimuli, J Exp Med. 192 (2000) 145-150.
35. R. Bhardwaj, J. Blanchard, Controlled-release delivery system for the alpha-MSH analog melanotan-I using poloxamer 407, J Pharm Sci. 85 (1996) 915-919.
36. S.C. Chi, H.W. Jun, Release rates of ketoprofen from poloxamer gels in a membraneless diffusion cell, J Pharm Sci. 80 (1991) 280-283.
37. J.Y. Chang, Y.K. Oh, H.G. Choi, Y.B. Kim, C.K. Kim, Rheological evaluation of thermosensitive and mucoadhesive vaginal gels in physiological conditions, Int J Pharm. 241 (2002) 155-163.
38. C.G. Park, C.A. Hartl, D. Schmid, E.M. Carmona, H.J. Kim, M.S. Goldberg, Extended release of perioperative immunotherapy prevents tumor recurrence and eliminates metastases, Sci Transl Med. 10 (2018).
39. A. Fakhari, M. Corcoran, A. Schwarz, Thermogelling properties of purified poloxamer 407, Heliyon. 3 (2017) e00390.
40. Y. Alkhatib, M. Dewaldt, S. Moritz, R. Nitzsche, D. Kralisch, D. Fischer, Controlled extended octenidine release from a bacterial nanocellulose/Poloxamer hybrid system, Eur J Pharm Biopharm. 112 (2017) 164-176.
41. E. Al-Ani, C. Martin, S.T. Britland, K. Doudin, D.J. Hill, The effect of the source and the concentration of polymers on the release of chlorhexidine from mucoadhesive buccal tablets, Saudi Pharm J. 27 (2019) 756-766.
42. Y. Yu, R. Feng, J. Li, Y. Wang, Y. Song, G. Tan, et al., A hybrid genipin-crosslinked dual-sensitive hydrogel/nanostructured lipid carrier ocular drug delivery platform, Asian J Pharm Sci. 14 (2019) 423-434.
43. Y.Z. Zhao, H.F. Lv, C.T. Lu, L.J. Chen, M. Lin, M. Zhang, et al., Evaluation of a novel thermosensitive heparin-poloxamer hydrogel for improving vascular anastomosis quality and safety in a rabbit model, PloS one. 8 (2013) e73178.
44. W.Y. Wang, P.C.L. Hui, E. Wat, F.S.F. Ng, C.W. Kan, C.B.S. Lau, et al., Enhanced Transdermal Permeability via Constructing the Porous Structure of Poloxamer-Based Hydrogel, Polymers. 8 (2016) 406-418.
45. M. Reth, Matching cellular dimensions with molecular sizes, Nature immunology. 14 (2013) 765-767.
46. S.D. Allison, Analysis of initial burst in PLGA microparticles, Expert Opin Drug Deliv. 5 (2008) 615-628.
47. O. Inal, E.A. Yapar, Effect of mechanical properties on the release of meloxicam from poloxamer gel bases, Indian J Pharm Sci. 75 (2013) 700-706.
48. K. Zhang, X. Shi, X. Lin, C. Yao, L. Shen, Y. Feng, Poloxamer-based in situ hydrogels for controlled delivery of hydrophilic macromolecules after intramuscular injection in rats, Drug Deliv. 22 (2015) 375-382.
49. T.P. Johnston, M.A. Punjabi, C.J. Froelich, Sustained delivery of interleukin-2 from a poloxamer 407 gel matrix following intraperitoneal injection in mice, Pharm Res. 9 (1992) 425-434.
50. W. Boonlai, V. Tantishaiyakul, N. Hirun, T. Sangfai, K. Suknuntha, Thermosensitive Poloxamer 407/Poly(Acrylic Acid) Hydrogels with Potential Application as Injectable Drug Delivery System, AAPS PharmSciTech. 19 (2018) 2103-2117.
51. Y. Mao, X. Li, G. Chen, S. Wang, Thermosensitive Hydrogel System With Paclitaxel Liposomes Used in Localized Drug Delivery System for In Situ Treatment of Tumor: Better Antitumor Efficacy and Lower Toxicity, J Pharm Sci. 105 (2016) 194-204.

52. A. Chenite, C. Chaput, D. Wang, C. Combes, M.D. Buschmann, C.D. Hoemann, et al., Novel injectable neutral solutions of chitosan form biodegradable gels in situ, Biomaterials. 21 (2000) 2155-2161.
53. S. Kim, S.K. Nishimoto, J.D. Bumgardner, W.O. Haggard, M.W. Gaber, Y. Yang, A chitosan/beta-glycerophosphate thermo-sensitive gel for the delivery of ellagic acid for the treatment of brain cancer, Biomaterials. 31 (2010) 4157-4166.
54. S.F. Khattak, S.R. Bhatia, S.C. Roberts, Pluronic F127 as a cell encapsulation material: utilization of membrane-stabilizing agents, Tissue Eng. 11 (2005) 974-983.
55. L.S. Yap, M.C. Yang, Evaluation of hydrogel composing of Pluronic F127 and carboxymethyl hexanoyl chitosan as injectable scaffold for tissue engineering applications, Colloids Surf B Biointerfaces. 146 (2016) 204-211.
56. H.H. Jung, K. Park, D.K. Han, Preparation of TGF-beta1-conjugated biodegradable pluronic F127 hydrogel and its application with adipose-derived stem cells, Journal of controlled release : official journal of the Controlled Release Society. 147 (2010) 84-91.
57. H. Parhiz, M. Khoshnejad, J.W. Myerson, E. Hood, P.N. Patel, J.S. Brenner, et al., Unintended effects of drug carriers: Big issues of small particles, Adv Drug Deliv Rev. 130 (2018) 90-112.
58. M.A. Westerink, S.L. Smithson, N. Srivastava, J. Blonder, C. Coeshott, G.J. Rosenthal, ProJuvant (Pluronic F127/chitosan) enhances the immune response to intranasally administered tetanus toxoid, Vaccine. 20 (2001) 711-723.
59. T. Ito, R. Amakawa, S. Fukuhara, Roles of toll-like receptors in natural interferon-producing cells as sensors in immune surveillance, Hum Immunol. 63 (2002) 1120-1125.
60. A. Iwasaki, R. Medzhitov, Toll-like receptor control of the adaptive immune responses, Nature immunology. 5 (2004) 987-995.
61. D. Xu, H. Liu, M. Komai-Koma, Direct and indirect role of Toll-like receptors in T cell mediated immunity, Cell Mol Immunol. 1 (2004) 239-246.
62. M.S. Akash, K. Rehman, H. Sun, S. Chen, Sustained delivery of IL-1Ra from PF127-gel reduces hyperglycemia in diabetic GK-rats, PloS one. 8 (2013) e55925.
63. J.K. Armstrong, H.J. Meiselman, T.C. Fisher, Inhibition of red blood cell-induced platelet aggregation in whole blood by a nonionic surfactant, poloxamer 188 (RheothRx injection), Thromb Res. 79 (1995) 437-450.
64. E.V. Batrakova, S. Li, Y. Li, V.Y. Alakhov, W.F. Elmquist, A.V. Kabanov, Distribution kinetics of a micelle-forming block copolymer Pluronic P85, Journal of controlled release : official journal of the Controlled Release Society. 100 (2004) 389-397.
65. N. Petrovsky, Comparative Safety of Vaccine Adjuvants: A Summary of Current Evidence and Future Needs, Drug Saf. 38 (2015) 1059-1074.
66. E. van Doorn, H. Liu, A. Huckriede, E. Hak, Safety and tolerability evaluation of the use of Montanide ISA51 as vaccine adjuvant: A systematic review, Hum Vaccin Immunother. 12 (2016) 159-169.
67. M.F. Fransen, R.A. Cordfunke, M. Sluijter, M.J. van Steenbergen, J.W. Drijfhout, F. Ossendorp, et al., Effectiveness of slow-release systems in CD40 agonistic antibody immunotherapy of cancer, Vaccine. 32 (2014) 1654-1660.
68. S. Bobbala, V. Tamboli, A. McDowell, A.K. Mitra, S. Hook, Novel Injectable Pentablock Copolymer Based Thermoresponsive Hydrogels for Sustained Release Vaccines, AAPS J. 18 (2016) 261-269.